

Research Paper—Physics



SEPT—2009

THE SPACE DENSITY OF QSOs



IROM ABLU MEITEI * K. YUGINDRO SINGH

*Department of Physics, Manipur University, Canchipur, Imphal

ABSTRACT

A study of the space density of the quasi-stellar objects (QSOs), as represented by their luminosity functions, and their evolution is carried out by using the 2 Degree Field QSO Redshift Survey (2QZ) 10k catalogue of the Anglo Australian Telescope ($q_0=0.5$, $H_0=100 \text{ km s}^{-1} \text{ Mpc}^{-1}$). The Monte Carlo Technique of numerical integration was used in determining a binned estimate of the QSO luminosity function for more than 10990 QSOs with $0.3 < z < 2.3$ for five redshift intervals. For each redshift range the luminosity function is found to exhibit a downturn at the fainter magnitudes. Such a downturn is also observed in the luminosity function of the QSOs in the hard x-ray region. Incompleteness of the optical surveys at the fainter magnitudes might have led to a sharper downturn. Taking those QSOs with absolute magnitude, $M_B < -22.5$, two smooth two-power-law functions, each having the form $\phi(L_B) \propto [(L_B/L_B^*)^\alpha + (L_B/L_B^*)^{-1}]^{-1}$ with a power law pure luminosity evolution of the form $L_B^*(z) \propto (1+z_m)^\alpha$, z_m being the mean redshift of the redshift interval, were used to fit separately the luminosity functions of the brighter and the fainter QSOs for each redshift interval. From a simple fitting of the QSO luminosity function we have estimated the best fit parameters.

PACS codes: 95.75.Pq, 95.80.+p, 95.85.Kr, 98.54.-h, 98.54.Cm

Key words—galaxies: active

Introduction—

The quasi-stellar object (QSO) being a subclass of the Active Galactic Nuclei (AGN), the QSO luminosity function and its evolution with redshift provide valuable information about how the population of the Active Galactic Nuclei evolves with time. And the QSO luminosity function at high redshifts provides important constraints on the ionizing UV radiation field of the early Universe [9]. The QSO luminosity function for those QSOs with $z < 2.2$ and $M_B < -23$ was modeled with a two-power-law function with a steeper bright end [$\phi(L_B) \propto$

$L_B^{-3.6 \pm 0.1}$] and a flatter faint end [$\phi(L_B) \propto L_B^{-1.2 \pm 0.1}$] along with a redshift dependence of the characteristic luminosity function (where the two power laws meet) of the form

$L_B^*(z) \propto (1+z)^k$; the value of k is found to be $\sim 3 \text{--} 4$ [1,2,6,8]. Exponential luminosity function evolution models, both as a function of the look-back time $L_B^*(z) \propto e^{k\tau}$ and as a second order polynomial $L_B^*(z) \propto 10^{f(z)}$, where $f(z) = k_1 z + k_2 z^2$, are found to provide acceptable fit to the data set comprising of the 2QZ and the Large Bright Quasar Survey [3,4].

In the present study we used the 2dF QSO Redshift Survey (2QZ) 10k catalogue QSOs

to determine a binned estimate of the QSO luminosity function and we studied the QSO luminosity function and its evolution for a $q_0=0.5$ universe. The Monte Carlo technique of numerical integration was used in the determination of the luminosity function. Using simple curve fitting techniques we have studied the QSO luminosity function and its evolution. Those QSOs with $z < 2.3$ and $M_B < -22.5$ were used. The absolute magnitude limit $M_B < -22.5$ is taken as the 2QZ survey becomes incomplete at the fainter magnitudes. Two smooth two-power-law functions with a power law pure luminosity evolution of the characteristic luminosity of the form $L_B^*(z) \propto (1+z_m)^k$, (z_m being the mean redshift of the redshift interval) are used to fit the luminosity function at the brighter and the fainter magnitudes separately and the values of the best fit parameters are found out.

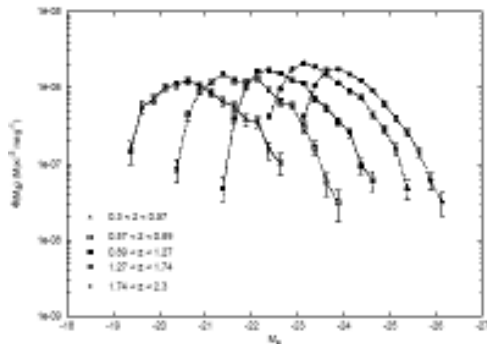


Fig 1 Luminosity function for the 2QZ 10k QSOs ($q_0=0.5$, $H_0=100 \text{ km s}^{-1} \text{ Mpc}^{-1}$)

2. Data

The 2QZ survey was carried out at the Anglo-Australian Telescope using the 2-degree Field multi-object spectroscopic system. It is flux limited in the b_j band. Magnitudes were determined from the Automatic Plate

Measuring scans of the UK Schmidt Telescope (UKST) photographic plates. The survey limits are $18.25 < b_j < 20.85$. Colour selection was made in the $u - b_j$ vs $b_j - r$ plane. We have studied the 2QZ 10k QSOs with $0.3 < z < 2.3$. The absolute magnitudes of these QSOs lie within the range -18.75 to -26.25 . As the survey is incomplete at the fainter magnitudes we have not incorporated those QSOs with $M_B > -22.5$ in the analysis for the QSO luminosity function. The 2QZ area comprises of two $75^\circ \times 5^\circ$ declination strips centred on $\alpha = 30^\circ$ and $\alpha = 0^\circ$. The $\alpha = 30^\circ$ strip extends from $\alpha = 21^h 40$ to $\alpha = 3^h 15$ in the South Galactic Cap and the equatorial strip extends from $\alpha = 9^h 50$ to $\alpha = 14^h 50$ in the North Galactic Cap (for details see [4]). The survey area of the 10k catalogue is 289.6 deg^2 (after corrections for the observational incompleteness).

3. Analysis and Results

The accessible comoving volume of each QSO (V_a^i) was computed and a binned estimate of the QSO luminosity function was found out in five redshift intervals for $q_0 = 0.5$ and $H_0 = 100 \text{ km s}^{-1} \text{ Mpc}^{-1}$ using the relation

$$\Phi(M_B, z) dM = \sum_{z_i \in (z_1, z_2), M_i \in (M_1, M_2)} \frac{1}{V_a^i} \tag{1}$$

where $z_i = z + dz/2$; $z_2 = z + dz/2$ and $M_1 = M + dM/2$; $M_2 = M + dM/2$.

The Poisson error is given by $\sigma = \sum_i [1/(V_a^i)^2]^{0.5}$ [5,6].

Those bins with less than five QSOs were neglected. The binned estimate of the QSO luminosity function in five redshift intervals is shown in Fig. 1. It is observed that for each redshift interval the luminosity function exhibits a downturn in the slope of the luminosity

function towards the faint end. The downturn is observed even at the magnitudes brighter than the cut-off magnitude $M_B < -22.5$. Such a downturn is also observed in the hard x-ray luminosity function of the QSOs (10). However the downturn is rather abrupt and occurs at comparatively brighter magnitudes in the case of the optical luminosity function. The optical

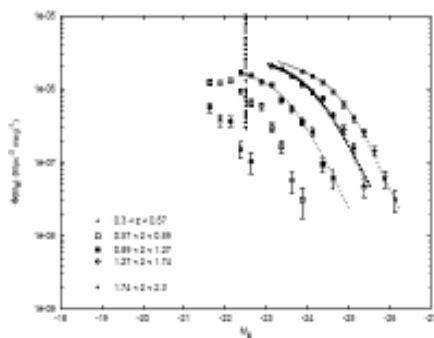


Fig 2 Luminosity function for the brighter 2QZ 10k QSOs (brighter in each redshift interval) ($q_0=0.5$, $H_0=100 \text{ km s}^{-1} \text{ Mpc}^{-1}$). The best fit curves are also shown. The line $M_B = -22.5$ is shown as a dotted vertical line.

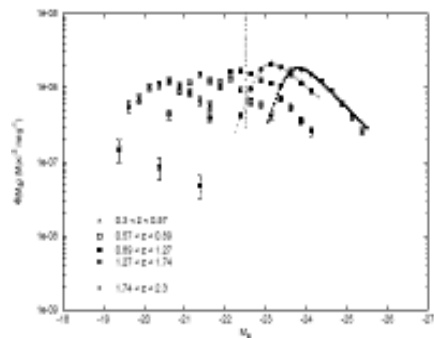


Fig 3 Luminosity function for the fainter 2QZ 10k QSOs (fainter in each redshift interval) ($q_0=0.5$, $H_0=100 \text{ km s}^{-1} \text{ Mpc}^{-1}$). The best fit curves are also shown. The line $M_B = -22.5$ is shown as a dotted vertical line.

probe might be missing some sources at the very lowest luminosities to which they probe (10). Also the downturn in the luminosity function for higher redshift comes at higher magnitudes. We fitted the QSO luminosity function for each redshift interval separately with two smooth two-power-law functions each of the form $\phi(L_B) \propto [(L_B/L_B^*)^\alpha + (L_B/L_B^*)^\beta]^{-1}$. For the QSOs brighter than the characteristic magnitude at fainter magnitudes, the smooth two-power-law function used is (in terms of absolute magnitude)

$$\Phi(M_B, z) = \frac{\Phi^*}{10^{0.4(M_B - M_B^*(z))(\alpha+1)} + 10^{0.4(M_B - M_B^*(z))(\beta+1)}}$$

where $M_B^*(z) = M_B^*(z=0) + 2.5 k \log_{10}(1+z_m)$, z_m being the mean redshift of each redshift interval. The best fitted luminosity functions for these QSOs are shown in Fig. 2. And the best fit values of the parameters are given in Table 1. For the fainter QSOs which are fainter than the characteristic magnitude at brighter magnitudes, a similar smooth two-power-law function is used:

$$\Phi(M_B, z) = \frac{\Phi^*}{10^{0.4(M_B - M_B^*(z))(\gamma+1)} + 10^{0.4(M_B - M_B^*(z))(\mu+1)}}$$

with similar evolution of the characteristic magnitude. The best fitted luminosity function of these QSOs are shown in Fig. 3 and the best fit values of the various parameters are given in Table 2. For Fig. 2, the best fit value of the parameter α is found to lie between “3.9 and “4.3. It is a little steeper than the value of 3.9 ± 0.15 reported by [2]. This may be due to the incompleteness of the survey about the brighter end for each redshift range leading to a drop in the luminosity function at the brighter end. The incompleteness at the brighter absolute magnitude for optical luminosity function is shown in [11]. The values of the parameters $\hat{\alpha}$ and k are roughly in agreement with the values

reported by [1,2,6]. The values of the parameter k found out in the present work are also in agreement with the values reported in these papers which use different survey data. It is also observed that the values of k for the fainter QSOs are generally a little larger than those of the brighter QSOs.

4. Conclusions—We have studied the luminosity function for 2QZ 10k QSOs with redshift $0.3 < z < 2.3$ and $M_B < -22.5$. It is observed that there is a downturn in the luminosity function at the fainter magnitudes for each redshift interval which is sharper than and more abrupt than the downturn observed in the hard x-ray luminosity function of the QSOs. Incompleteness of the survey, which

depends not only on the absolute magnitude, but also on the redshift, may be responsible for the sharper and more abrupt downturn in the luminosity function at the fainter magnitudes and also for the steeper slope towards the brighter end of the luminosity function.

Acknowledgements—The 2dF QSO Redshift Survey (2QZ) was compiled by the 2QZ survey team from observations made with the 2-degree Field on the Anglo-Australian Telescope. We are indebted to Dr. Ranjeev Misra and Prof. A. K. Kembhavi of IUCAA, Pune. We are grateful to the virtual observatory-India (vo-i). Irom Ablu Meitei acknowledges the CSIR for providing financial assistance as a Senior Research Fellow.

Table 1: Best fit values of the parameters of the luminosity function for the 2QZ 10k QSOs corresponding to Fig. 2 ($q_0 = 0.5$, $H_0 = 100 \text{ km s}^{-1} \text{ Mpc}^{-1}$)

z interval	α	β	k	M_B^*	ϕ^*	χ^2
0.89<z<1.27	$^{-}3.90 \pm 0.88$	$^{-}1.25 \pm 0.38$	3.5 ± 0.51	$^{-}20.72$	1.37×10^{-6} $\pm 7.64 \times 10^{-7}$	3.99×10^{-8}
1.27<z<1.74	$^{-}3.90 \pm 0.93$	$^{-}1.35 \pm 0.43$	3.5 ± 0.48	$^{-}20.72$	1.61×10^{-6} $\pm 1.0 \times 10^{-6}$	7.02×10^{-8}
1.74<z<2.3	$^{-}4.30 \pm 0.42$	$^{-}1.45 \pm 0.17$	3.5 ± 0.13	$^{-}20.72$	1.22×10^{-6} $\pm 3.17 \times 10^{-7}$	9.97×10^{-8}

Table 2: Best fit values of the parameters of the luminosity function for the 2QZ 10k QSOs corresponding to Fig. 3 ($q_0 = 0.5$, $H_0 = 100 \text{ km s}^{-1} \text{ Mpc}^{-1}$)

z interval	γ	μ	k	M_B^*	ϕ^*	χ^2
1.27<z<1.74	3.47 ± 0.11	$^{-}2.18 \pm 0.03$	4.39 ± 0.01	$^{-}18.50$	3.50×10^{-6} $\pm 4.19 \times 10^{-8}$	4.62×10^{-8}
1.74<z<2.3	3.37 ± 0.49	$^{-}2.38 \pm 0.11$	4.24 ± 0.03	$^{-}18.50$	3.22×10^{-6} $\pm 1.43 \times 10^{-7}$	4.32×10^{-8}

REFERENCE

[1] Boyle B. J., Fong R., Shanks T., Peterson B. A., MNRAS 227, 717 (1987) [2] Boyle B. J., Shanks T., Peterson B. A., MNRAS 235, 935 (1988) [3] Boyle B. J., Shanks T., Croom S. M., Smith R. J., Miller L., Loaring N., Heymans C., MNRAS 317, 1014 (2000) [4] Croom S. M., Smith R. J., Boyle B. J., Shanks T., Miller L., Outram P. J., Loaring N. S., MNRAS 349, 1397 (2004) [5] Croom S. M., Smith R. J., Boyle B. J., Shanks T., Loaring N. S., Miller L., Lewis I. J., MNRAS 322, L29 (2001) [6] Hartwick F. D. A., Schade D., ARA&A, 28,437 (1990) [7] Irom Ablu Meitei and K. Yugindro Singh Indian J. Physics 82(5),147 (2008) [8] Lampton M., Margon B., Bowyer S., ApJ, 208, 177 (1976) [9] Marshall H. L., ApJ, 299, 109 (1985) [10] Hunt M. P., Steidel C. C., Abelberger K. L., Shapley A. E., ApJ 605, 625 (2004) [11] Barger A. J., Cowie L. L., Mushotzky R. F., Yang Y., Wang W. H., Steffen A. T., Capak P., AJ, 129, 578 (2005) [12] Richards et al MNRAS, 360, 839 (2005) [13] B. M. Peterson: An Introduction to Active Galactic nuclei, Cambridge University Press [14] A. K. Kembhavi and J. V. Narlikar: Quasars and Active Galactic Nuclei, Cambridge University Press